Geoscience Frontiers 10 (2019) 1371–1381

HOSTED BY

ELSEVIER

Contents lists available at ScienceDirect

China University of Geosciences (Beijing)

Geoscience Frontiers

journal homepage: www.elsevier.com/locate/gsf

Research Paper

Assessing volcanic origins within detrital zircon populations – A case study from the Mesozoic non-volcanic margin of southern Australia

Milo Barham [a,*], Christopher L. Kirkland [a], Martin Danišík [b]

[a] *Centre for Exploration Targeting (CET) - Curtin Node, The Institute for Geoscience Research (TIGeR), School of Earth and Planetary Sciences, Curtin University, GPO Box U1987, Perth, WA 6845, Australia*

[b] *GeoHistory Facility, John de Laeter Center, Curtin University, GPO Box U1987, Perth, WA 6845, Australia*

ARTICLE INFO

Article history:
Received 14 March 2018
Received in revised form
10 November 2018
Accepted 14 January 2019
Available online 23 February 2019
Handling Editor: Nick M W Roberts

Keywords:
Provenance
Grain history
Thermochronology
Geochronology
Source to sink
Trace-elements

ABSTRACT

Detrital zircon U/Pb geochronology is a common tool used to resolve stratigraphic questions, inform basin evolution and constrain regional geological histories. In favourable circumstances, detrital zircon populations can contain a concomitant volcanic contribution that provides constraints on the age of deposition. However, for non-volcanic settings, proving isolated detrital zircon grains are from contemporaneous and potentially remote volcanism is challenging. Here we use same grain (U–Th)/He thermochronology coupled with U/Pb geochronology to identify detrital zircon grains of contemporary volcanic origin. (U–Th)/He ages from Cretaceous zircon grains in southern Australia define a single population with a weighted mean age of 104 ± 6.1 Ma, indistinguishable from zircon U/Pb geochronology and palynology (~104.0–107.5 Ma). Detrital zircon trace-element geochemistry is consistent with a continental signature for parent rocks and coupled with detrital grain ages, supports derivation from a >2000 km distant early- to mid-Cretaceous Whitsunday Volcanic Province in eastern Australia. Thus, integration of biostratigraphy, single-grain zircon double-dating (geochronology and thermochronology) and grain geochemistry enhances fingerprinting of zircon source region and transport history. A distal volcanic source and rapid continental-scale transport to southern Australia is supported here.

1. Introduction

Detrital zircon U/Pb geochronology has expanded to become a standard tool in the geosciences, permitting a diverse array of geological questions to be addressed. Proliferation of detrital zircon based provenance studies has allowed refinement of basin settings (Cawood et al., 2012), paleogeography, stratigraphy, as well as denudation histories (Sircombe and Freeman, 1999; Cawood et al., 2003; Fedo et al., 2003; Rahl et al., 2003; Veevers et al., 2005; Kirkland et al., 2007; Cecil et al., 2010; Dickinson and Gehrels, 2010; Gehrels, 2014; Fielding et al., 2017; Barham et al., 2018; Olierook et al., 2019). Of particular importance in detrital zircon studies is the date of the youngest component, which provides a maximum age for sediment deposition (maximum depositional age–MDA; Dickinson and Gehrels, 2009; Spencer et al., 2016). In volcanically active regions, large volumes of volcanogenic material can be shed into adjacent depocentres, providing excellent opportunities to constrain depositional ages through identification of the youngest volcanic zircon population, or more ideally, discrete tuff horizons (Rasmussen and Fletcher, 2010; Pointon et al., 2012, 2014; Metcalfe et al., 2015; Laurie et al., 2016; Mory et al., 2017). However, many depositional basins form in non-volcanic settings (e.g. intracontinental basins and post-rift passive margins), where U/Pb zircon geochronology may provide little constraint on depositional age (e.g., Cawood et al., 2012). In non-volcanic settings, recognition of dispersed contemporaneous volcanic zircon crystals cannot rely on the same traditional techniques employed in analysis of more proximal volcaniclastic successions (Fisher, 1961; Fisher and Schmincke, 1984; Heiken, 1985; Suthren, 1985) or defined tuff horizons (e.g., Schmitz, 2012). Consequently, the significance of distal and volumetrically minor contemporary volcanic zircon grains is often not fully realised.

Despite being a powerful tool, problems can arise with interpretation of detrital zircon U/Pb datasets when the ages of crystalline sources from disparate regions are the same (Rahl et al.,

---

* Corresponding author.
E-mail address: milo.barham@curtin.edu.au (M. Barham).
Peer-review under responsibility of China University of Geosciences (Beijing).

https://doi.org/10.1016/j.gsf.2019.01.003

2003; Campbell et al., 2005; Reiners et al., 2005; Spencer et al., 2016; Barham et al., 2018). Several geochemical signatures within zircon grains (Lu–Hf, trace-elements and O-isotopes) can help to uniquely distinguish ultimate crystalline source regions. However, establishing the degree of complexity in the exhumation history and sedimentary routing of grains, particularly where both direct sourcing and recycling through intermediate sediment reservoirs are possible, is more problematic. Recently, individual zircon grain shape has been suggested to retain information with respect to provenance and routing mechanisms (Markwitz et al., 2017; Makulini et al., 2018; Markwitz and Kirkland, 2018). However, in order to more fully investigate zircon grain origin, exhumation pathways and subsequent transport processes, an integrated "double-dating" approach, combining U/Pb with (U–Th)/He dating techniques (applied to the same grain) has proven to be a useful tool (Rahl et al., 2003; Campbell et al., 2005; Reiners et al., 2005; Saylor et al., 2012; Xu et al., 2017). This approach offers a means to access information not only on the time of zircon crystallisation recorded by the high-temperature U/Pb geochronometer, but also on the previously inacessible post-crystallisation history of zircon grains that can be revealed by the (U–Th)/He system as it charts cooling through the ~180 °C isotherm (Reiners et al., 2004). Although this closure temperature is relatively low, potentially resulting in widespread re-setting of zircon grains that had experienced distinct histories up to that point, the integration of thermochronology data with crystallisation age information in the context of regional geology, can still provide diagnostic grain history information (Reiners et al., 2005).

Recent work on an enigmatic Cretaceous zircon subpopulation within a detrital zircon sample recovered from drillcore in southern Australia (Madura Shelf; Barham et al., 2016, 2018) suggested extreme (>1000 km) grain dispersal from explosive eruptions on the eastern margin of Gondwana during the mid-Cretaceous for the young Albian zircon component (Fig. 1). An alternative grain history involving more protracted recycling and fluvial transport was proposed for detrital zircon grains with indistinguishable U/Pb age and Hf-isotope compositions from younger Upper Cretaceous (Santonian-Maastrichtian) sediments of the Ceduna Subbasin, further east on Australia's southern margin (Fig. 1; Lloyd et al., 2016; Veevers et al., 2016). Local rift-related volcanism along the southern margin has also been proposed as a more direct and proximal source of middle-Cretaceous volcanic-derived sedimentary rock offshore of southeast Australia (Gleadow and Duddy, 1981; Felton, 1992), as well as suggested as a more plausible recycled source for Cretaceous zircon grains from the Ceduna Subbasin (MacDonald et al., 2013). Although local southern margin rift volcanism is significantly undermined by a lack of evidence for appropriately aged volcanic rocks, as well as geochemical and sedimentological data (Bryan et al., 1997; Constantine, 2001), the idea persists, and has even been expanded to encompass the broader Bight Basin (Fig. 1; Duddy, 2016). Consequently, this work sets out to test these distinct hypotheses, and demonstrate the

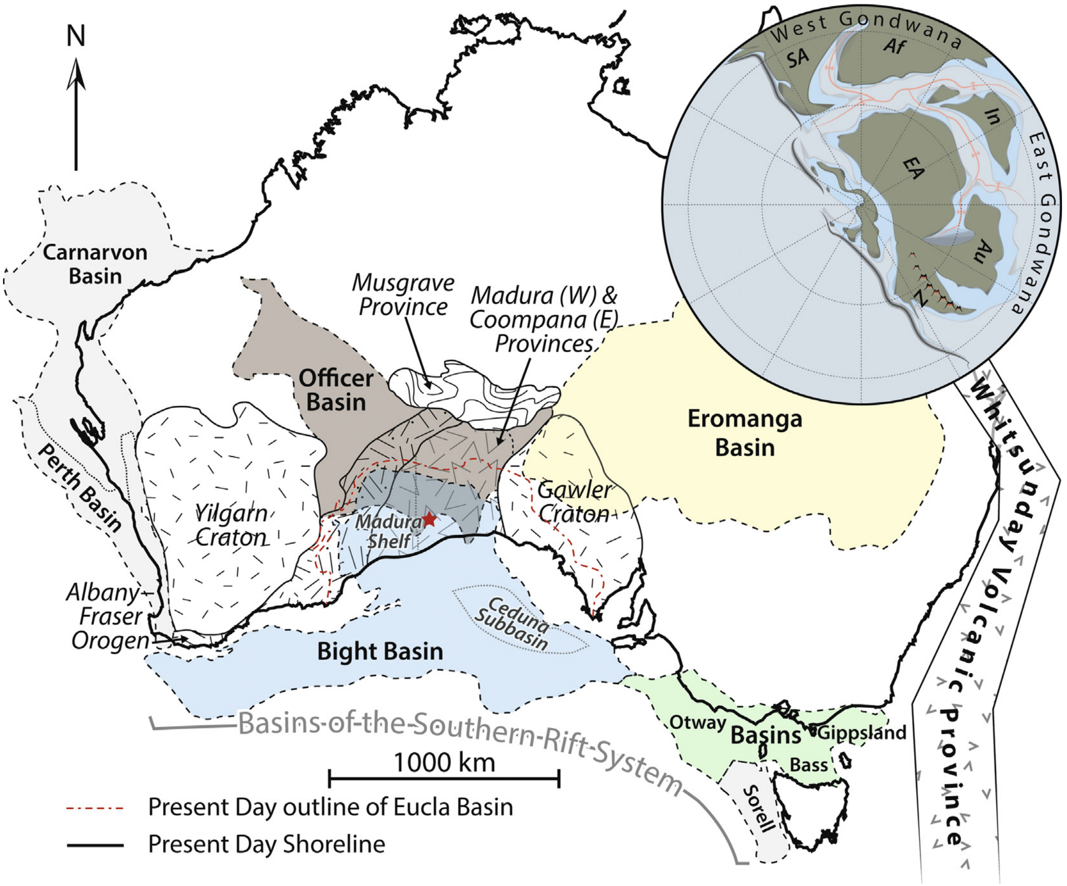

Figure 1. Simplified map of key geological regions associated with the study. Sedimentary basins mentioned in the text highlighted in pastel colours. Crustal blocks indicated with filled ornament. The Madura Shelf and Ceduna Subbasin form part of the larger Bight Basin. Red star indicates the location of FOR011 borehole from which sample 199453 was taken. The extent of overlying Cenozoic carbonates is shown by the red outline of the Eucla Basin. Composite map with elements from Bryan et al. (1997) and Barham et al. (2018). Inset map shows a reconstruction of the paleogeography in the middle-Cretaceous with the view centred on the south pole; note volcanic system in eastern Australia, red lines correspond to spreading ridges, SA–South America, Af–Africa, In–India, EA–East Antarctica, Au–Australia, Z–Zealandia; modified from Blakey (2008).

utility of integrated same-grain geochronology-thermochronology-geochemistry techniques in instances of more enigmatic zircon subpopulations recovered during standard zircon provenance studies. We apply a U/Pb and (U–Th)/He double-dating approach to establish whether (i) rapid cooling occurred near contemporaneously with zircon crystallisation as would be consistent with an eruptive volcanic origin, or (ii) if there was a more protracted cooling history, as would be the case for a plutonic zircon crystal that was eroded from deeper igneous plumbing and transported by more traditional surface fluvial processes, and (iii) whether any low- to moderate-temperature thermal events associated with burial in intermediate sediment sequences hosting the detrital zircon could be identified, helping to constrain grain histories and the mechanism by which the grains were incorporated into their current position. Geochronological data are combined with biostratigraphical data and trace-element discrimination of parent source-rock tectonic setting, to refine the primary origin of the detrital grains and establish a more complete source to sink history.

2. Geological background

Australia records a protracted history of rifting from eastern Gondwana, with the Perth Basin that developed between India and Australia exhibiting several discrete extensional episodes through the Phanerozoic from mid-Paleozoic to final rupture in the Cretaceous (Playford et al., 1976; Olierook et al., 2015, 2016, 2019). Final break-up and isolation of Australia occurred in the Mesozoic (Fig. 1; Blakey, 2008; Seton et al., 2012). Separation occurred earliest on Australia's aforementioned western margin and propagated eastwards between Australia and Antarctica (Blevin and Cathro, 2008; Gibbons et al., 2013; Olierook et al., 2016). Consequent crustal thinning on the southern margin of Australia formed a series of broadly coastline-parallel elongate basins, subbasins and intervening platforms that constitute the broader Southern Rift System (Stagg et al., 1990). The Bight Basin constitutes the largest component of the Southern Rift System, extending over 2000 km of the southern margin of Australia (Fig. 1; Totterdell and Bradshaw, 2004). Further east, the Otway, Gippsland and Bass basins record development under different extension directions, as well as distinct lithostratigraphic units recording contemporary intermediate-felsic, volcanic-derived sedimentation in the mid-Cretaceous (Blevin and Cathro, 2008). Despite the presence of substantial volumes of volcanogenic sedimentary material (andesitic, dacitic and rhyolitic lithic components) within the southeastern Australian basins (interpreted as externally sourced from the east; Bryan et al., 1997), the broader southern margin of Australia is considered a non-volcanic rifted margin (Direen et al., 2007, 2011; Meeuws et al., 2016). This is in contrast to northwestern and eastern Australian margins that are volcanic (Bryan et al., 1997; Mihut and Müller, 1998; Menzies et al., 2002; Direen et al., 2008), and whose basins commonly host volcanic products (both intrusive and extrusive igneous rocks, and eruptive volcaniclastics).

As a result of the Cretaceous eustatic high, widespread deposition was simultaneously recorded across low-lying areas of Australia, in particular across the Madura Shelf (northern Bight Basin) and the Great Australian Basin (including the Eromanga Basin; Fig. 1). Cretaceous thermal subsidence and transgression of the Madura Shelf drove evolution from fluvio-lacustrine (Loongana Formation) to marine-shelf (Madura Formation) environments (Lowry, 1970; Haq, 2014; Barham et al., 2018). Fully marine conditions were established across the Madura Shelf by the Albian (middle-Cretaceous) with deposition of fossiliferous glauconitic fine sands and silts of the Madura Formation sampled here. Coevally, interplay of sediment supply, dynamic topography and, significantly, eustasy saw evolution of shallow marine to fluvial environments recorded in the Eromanga Basin in northeast Australia from the early- to mid-Cretaceous (Gallagher and Lambeck, 1989; Gallagher et al., 1994; Matthews et al., 2011; Müller et al., 2016).

Sediments within the Eromanga Basin are associated with widespread explosive volcanism preceding continental rupture and ultimate rifting of Zealandia from eastern Australia (Whitsunday Volcanic Province) during the Late Cretaceous (Bryan et al., 2012). Within the Whitsunday Volcanic Province, lithologies range from mafic to felsic compositions and are volumetrically dominated by welded dacitic–rhyolitic and relatively lithic-rich ignimbrite units (up to 1 km thick) associated with relatively large caldera vestiges (tens of kilometers) that attest to explosive activity (Bryan et al., 1997, 2012). Greater than 2×10^6 km^3 of volcaniclastic material derived from the Whitsunday Volcanic Province were supplied to eastern Australian sedimentary basins (principally the Eromanga Basin within the Great Australian Basin; Bryan et al., 2012) and later recycled into the Upper Cretaceous Ceduna Delta in the Ceduna Subbasin within the eastern Bight Basin (Fig. 1; Lloyd et al., 2016; Veevers et al., 2016). Importantly, interpreted volcanic Albian aged zircon grains with essentially identical U/Pb ages and Hf-isotope values are identified in the Eromanga Basin (Bryan et al., 1997; Greentree, 2011; Tucker et al., 2016), the upper Ceduna Delta lobe (MacDonald et al., 2013; Lloyd et al., 2016; Veevers et al., 2016) and in a single sample of the Madura Shelf studied here (Barham et al., 2016). Similarly-aged volcanic detritus is also reported from the Otway Basin in SE Australia (Gleadow and Duddy, 1981; Felton, 1992).

3. Samples and methods

Zircon grains used in this study were separated from a 1 kg sample of friable, fine-medium glauconitic, micaceous sandstone (199453) collected at a depth of 98 m in borehole FOR011 (Fig. 1). New (U–Th)/He and additional trace-element geochemistry analyses were undertaken on zircon grains previously mounted and ablated for U/Pb geochronology and Hf-geochemistry (Barham et al., 2016). For (U–Th)/He dating, we selected zircon grains previously dated (i.e. same-grain double-dating) using U/Pb geochronology and identified as an Albian, ~106 Ma "volcanic" component (Fig. 2), as well as grains interpreted to be from Mesoproterozoic basement (Table 1; Barham et al., 2016). The grains within error or U/Pb concordia ages were plucked out from the "mount 2" of Barham et al. (2016) and analysed following the (U–Th)/He dating procedure in Danišík et al. (2012) and detailed in Appendix A. Details of the trace element analysis by LA-ICPMS techniques are provided in Appendix A.

4. Results

U/Pb and Hf-isotope data from the dominantly regionally-sourced (Meso-Paleoproterozoic basement) detrital zircon population recovered are presented and discussed in detail in Barham et al. (2016, 2018), with the focus here on investigating the distinct Albian subpopulation (~15% of the total concordant population of 252 analyses) that constrains the MDA of the sample.

4.1. (U–Th)/He thermochronology

Zircon (U–Th)/He ages (ZHe) determined for eight crystals representing the Albian zircon population range from 92.5 ± 7.6 Ma to 111.1 ± 9.2 Ma (1σ; Table 1, Figs. 3 and 4). All ages overlap within 2σ uncertainty and define a Gaussian population with a weighted mean of 104 ± 6.1 Ma (MSWD = 0.62). In contrast, two zircon

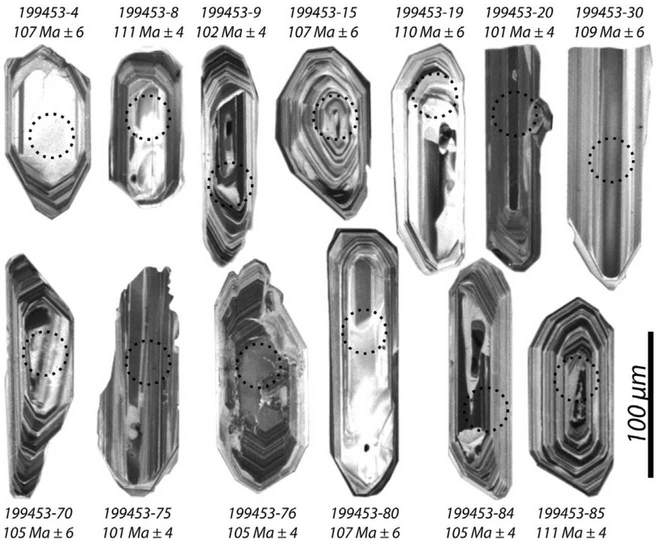

Figure 2. Representative cathodoluminescence images of Albian zircon grains analysed. Sample numbers and U/Pb Concordia ages provided in italics. Dotted circles indicate the location of the laser ablation pits.

crystals interpreted as deriving from Proterozoic basement yield ZHe ages of 478.1 ± 39.7 Ma and 737.1 ± 60.4 Ma (1σ) that are significantly younger than their U/Pb crystallisation age (1.7 Ga; Table 1, Fig. 4).

4.2. Trace-element geochemistry

Zircon trace element geochemistry is increasingly being used as a tool to identify crustal-scale to local metamorphic and magmatic processes operating during grain crystallisation, and further distinguish zircon provenance (Belousova et al., 2002; Grimes et al., 2007, 2015; Chapman et al., 2016; McKenzie et al., 2018). A REE plot of ~106 Ma grains reveals consistent geochemical profiles with a typical positive slope where HREE is enriched relative to LREE, consistent with REE incorporation controlled by lattice strain (Fig. 5; Blundy and Wood, 1994). The LREE are moderately flat, with a positive Ce anomaly and negative Eu anomaly, likely controlled by magma oxidation state (Trail et al., 2012). $(Lu/Gd)_N$ ranges from 16 to 102, indicating moderate to steep HREE patterns. The Albian zircon grains overlap the majority of detrital zircon grains from the Madura Shelf sample and fall in the continental field on a U/Yb versus Y plot (Fig. 6; Grimes et al., 2007). All but one Albian zircon grain plot exclusively within the continental crust field. Numerous detrital zircon grains and a single Albian grain plot with higher Y and lower U/Yb values within the overlap of the continental and oceanic crust fields, while one detrital grain lies completely within the oceanic crust field (Fig. 6).

5. Discussion

5.1. Current data and hypotheses

Three conflicting pathways have been proposed to explain delivery of Albian zircon grains to Cretaceous successions on the southern margin of Australia.

(i) Contemporaneous volcanism argued to be a cryptic feature of Australia's southern margin rift system, with proximal volcanic centers invoked to explain the abundance and coarseness of apparently unaltered labile volcanic mineral phases in mid-Cretaceous sequences in offshore south-eastern Australian Basins (Gleadow and Duddy, 1981; Felton, 1992; Duddy, 2003). Despite significant criticisms (see Bryan et al., 1997) and an absence of evidence for appropriately aged volcanism on the margin (Meeuws et al., 2016), Mesozoic volcanism has been invoked more widely across the southern margin to explain young zircon populations in the Ceduna Subbasin (MacDonald et al., 2013), as well as recently being proposed for material recovered from the Madura Shelf (Duddy, 2016).

(ii) Continental-scale alluvial-fluvial transport from a large volcanic system developed along the eastern margin of Australia (Whitsunday Volcanic Province), either directly or via recycling through intermediate sediment storage areas is supported by sedimentology (paleocurrents and facies relationships) and detrital zircon age and Hf-isotope similarity for material within the Ceduna Subbasin (Lloyd et al., 2016; Veevers et al., 2016).

(iii) Extreme dispersal of zircon grains into the catchment of the Madura Shelf by super-volcanic eruptions on the eastern margin of Australia (Barham et al., 2016). Zircon Hf-isotopes and U/Pb ages corresponding with the Whitsunday Volcanic Province, which is increasingly being recognized for the large magnitude of its explosive nature and voluminous volcaniclastic deposits, are also compatible with this interpretation (Ewart et al., 1992; Bryan et al., 1997, 2000, 2010, 2012; Pirajno

Table 1
Associated geochronological data table for (U-Th)/He dated zircon grains from sample 199453 on the Madura Shelf, Western Australia. Crystal numbers are consistent with those used in Barham et al. (2016).

Crystal #	Interpreted source	U/Pb age (Ma)	±2σ (Ma)	^{232}Th (ng)	± (%)	^{238}U (ng)	± (%)	^{147}Sm (ng)	± (%)	^{4}He (ncc)	± (%)	TAU (%)	Th/U	eU (ppm)	Raw He age (Ma)	±2σ (Ma)	Ft	± (%)	Cor. He age (Ma)	±2σ (Ma)
8*	basement	**1729**	66	0.123	1.5	0.184	1.9	0.0028	25.0	15.861	0.7	1.8	0.67	199	579.4	20.8	0.79	8	737.1	120.8
94*	basement	**1655**	90	0.096	2.0	0.146	2.4	0.0009	44.6	7.448	0.7	2.2	0.65	102	351.9	15.4	0.74	8	478.1	79.4
71	volcanic	**111**	10	0.189	1.5	0.248	1.9	0.0004	49.6	2.470	0.7	1.7	0.76	208	69.1	2.4	0.75	8	**92.5**	15.2
116	volcanic	**111**	12	0.410	1.5	0.629	1.9	0.0021	37.6	6.901	0.7	1.8	0.65	482	77.7	2.8	0.70	8	**110.5**	18.2
101	volcanic	**102**	10	0.339	2.0	0.536	2.4	0.0022	37.1	6.023	0.8	2.2	0.63	479	79.9	3.6	0.72	8	**111.1**	18.4
88	volcanic	**106**	14	0.239	1.5	0.308	1.9	0.0005	48.9	3.386	0.7	1.7	0.77	347	76.1	2.6	0.77	8	**98.7**	16.2
108	volcanic	**113**	12	0.305	1.5	0.443	1.9	0.0018	39.2	5.611	0.7	1.8	0.68	491	89.0	3.2	0.83	8	**107.1**	17.6
41	volcanic	**106**	10	0.445	2.0	0.661	2.4	0.0032	25.5	7.855	0.7	2.2	0.67	391	83.8	3.6	0.79	8	**106.6**	17.6
39	volcanic	**105**	8	0.113	1.5	0.155	1.9	0.0039	25.3	1.857	0.8	1.8	0.72	177	83.6	3	0.77	8	**108.5**	17.8
64	volcanic	**102**	16	0.097	1.5	0.101	1.9	0.0009	40.9	1.233	0.9	1.8	0.95	120	81.1	3	0.79	8	**103.2**	17

Source – source rock and U/Pb concordia ages according to Barham et al. (2016); TAU – total analytical uncertainty; eU – effective Uranium; Raw He age – (U–Th)/He age uncorrected for alpha recoil; Ft – alpha recoil correction factor after Farley et al. (1996) corrected for the mineral portion removed by polishing; Cor. He age – (U–Th)/He age corrected for alpha recoil. Average age for the population of young zircon crystals was calculated as error weighted average using Isoplot Excel Add-in (Ludwig, 2012); 95% Confidence Interval is the error propagated from the assigned data-point errors multiplied by the square root of the MSWD and Student's-t for N-1 degrees of freedom. Zircon crystals from the Mesoproterozoic basement (marked with an asterisk) were not included in the weighted mean calculation.

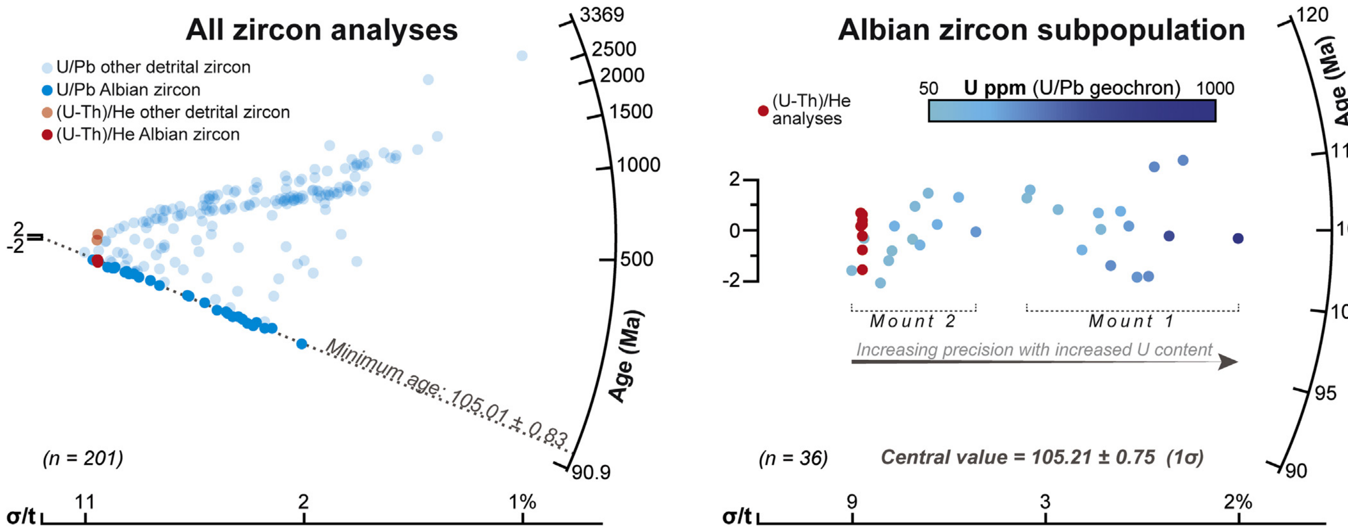

Figure 3. U–Pb and (U–Th)/He datasets of detrital zircon analyses plotted on a logarithmically scaled radial plot (Galbraith, 1988, 1990) constructed using RadialPlotter v. 9.0 (Vermeesch, 2009). The relative age uncertainty of each analysis can be found by applying the 2σ vertical scale bar (left) to each data point and projecting from the origin through the extremes of the 2σ scale to the age scale arc.

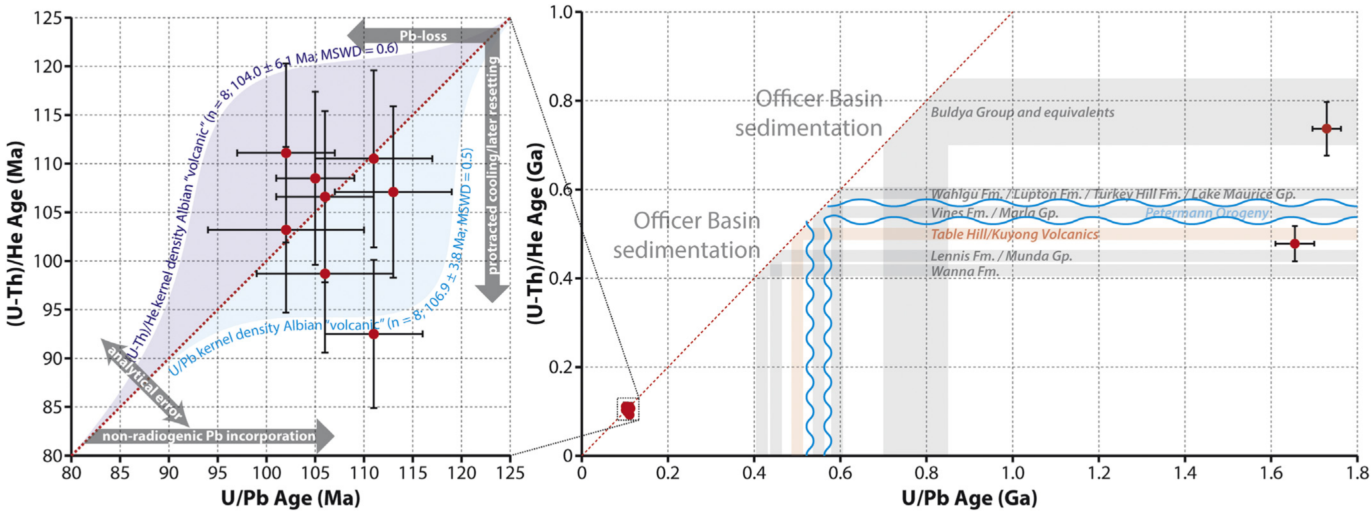

Figure 4. Biplot of (U–Th)/He vs. U/Pb ages for zircon grains analysed here from sample 199453. Kernel density functions provided in the enlargement for both (U–Th)/He (purple) and U/Pb (blue) ages of double dated Albian zircon grains. Transparent coloured bars on the main plot indicate intervals of sequence accumulation within the Officer Basin. Error bars plotted at a 1σ level.

and Hoatson, 2012). Additionally, the relatively distinct grain shape of the Albian zircon population may be consistent with this pathway, dissimilar to associated older detrital zircon grains within the population (Fig. 2; see Markwitz et al., 2017; Makulini et al., 2018; Markwitz and Kirkland, 2018).

Palynomorphs recovered (Barham et al., 2016) from adjacent sampling of the Madura Formation within the FOR011 core attributed to the *Pseudoceratium* [*Endoceratium*] *ludbrookiae* zone of Helby et al. (1987), independently constrain the age of deposition to ~104–107.5 Ma (Partridge, 2006). This age is consistent with palynostratigraphy in regionally adjacent wells (Totterdell and Krassay, 2003) and in good agreement with the Concordia U/Pb age (~106 Ma) of the youngest zircon component in sample 199453, implying rapid incorporation of this age subpopulation to the Madura Shelf sequence. In contrast to this, similarly aged Albian detrital zircon grains recovered from the Ceduna Subbasin, are significantly older than the depositional age of their host sediments (Coniacian–Maastrichtian), implying a more protracted transport history in processes quite distinct from those inferred for the Madura Shelf subpopulation (Barham et al., 2016). Currently no older (Albian) material is available from the Ceduna Delta to assess the presence or absence of Albian zircon grains and the nature of their transport. Disparities in the overall detrital zircon population age characteristics (Barham et al., 2018), as well as landscape evolution modelling (Salles et al., 2017), imply a disconnect between the sedimentary systems of the Madura Shelf and those of the Eromanga Basin and Ceduna Subbasin. The majority of detrital zircon grains from the Madura Shelf and regional overlying Cenozoic clastics match (Meso-Paleoproterozoic) hinterland crystalline rocks of the Albany-Fraser Orogen (west) and Musgrave Province (north), as well as underlying basement of the Madura and Coompana Provinces (Fig. 1; Hou et al., 2011; Reid et al., 2013; Barham et al., 2018; Makulini et al., 2018), while distinctive eastern

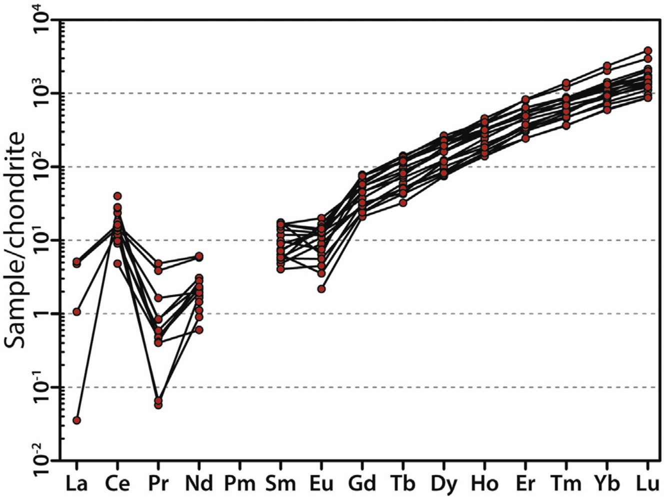

Figure 5. Chondrite-normalised (Boynton, 1984) trace-element spider diagram of Albian zircon grains from the Madura Formation (sample 199453).

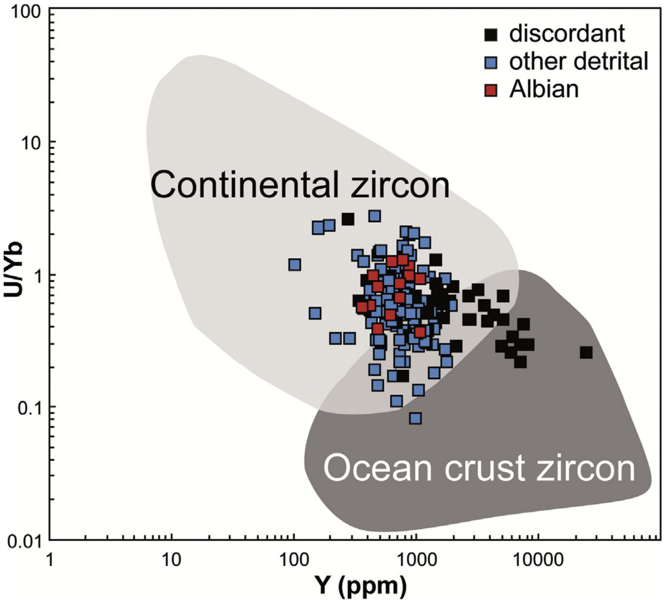

Figure 6. Trace element discrimination diagram for detrital zircon grains in sample 199453, Madura Formation. Fields after Grimes et al. (2007). Uncertainty obscured within the symbol used for each point.

Australian source regions are expressed in the detrital zircon populations of the Ceduna Subbasin (Neoproterozoic to Phanerozoic) and Eromanga Basin (Greentree, 2011; MacDonald et al., 2013; Tucker et al., 2013, 2016; Veevers et al., 2016). Thus, the distinct but subordinate Albian zircon population has been interpreted as reworked into local Madura Shelf clastic sediments only after significant aerial dispersion into the Madura Shelf catchment (Barham et al., 2016, 2018).

5.2. Establishing a volcanic origin based on integrated U/Pb geochronology and (U–Th)/He thermochronology

Identifying the youngest zircon age component (MDA) and determining the length of time between its crystallisation, exposure to the surface and ultimate incorporation into a sediment is critical for any volcanic interpretation of a distinct detrital zircon subpopulation. However, establishing the precise timing of these different steps may be significantly influenced by the dating techniques applied. Despite larger uncertainties potentially masking magma chamber processes operating on $\ll 1$ Ma timescale (autocrystic vs antecrystic grains, magma residence, heterogeneous cooling, etc.; Sano et al., 2002; Buret et al., 2016; Mami et al., 2017), *in situ* LA-ICPMS remains the standard for detrital provenance studies and has been demonstrated capable of resolving distinct episodes of pluton growth in the world's youngest exposed plutonic rocks (Ito et al., 2017; Spencer et al., 2019). Such age resolution is achieved through statistical, error-weighted assessment of discrete population ages. Thus, by using (i) cathodoluminescence to constrain crystallisation histories (Fig. 2; Corfu et al., 2003), (ii) selective analytical spot placement, and (iii) combined age and geochemistry to define unique populations (c.f. Gagnevin et al., 2010), to demonstrate genetic groups, statistical population ages with MSWD (mean squared weighted deviation) information can demonstrate more refined event ages from LA-ICPMS data (as well as the level of age confidence). This approach, applied to the Albian zircon subpopulation analysed here argues against significantly distinct events being represented (Barham et al., 2016). Although closely spaced (~100 ka) zircon growth phases or eruptive events cannot be resolved, their distinction is irrelevant for the purpose of this study.

Temporal concordance of zircon (U–Th)/He and U/Pb ages is important for demonstrating geologically instantaneous cooling of the grains (rapid transition from magma chamber to the surface and availability to sedimentary processes) and lack of subsequent burial resetting events (protracted detrital grain history; Xu et al., 2017). However, typical age population plotting techniques combine data regardless of precision, potentially concealing data complexity (e.g., Vermeesch, 2012). In order to simultaneously visualise zircon (U–Th)/He and U/Pb datasets whilst being mindful of their respective precisions, we propose that radial plots (Galbraith plots) are a powerful graphing technique that can meaningfully assess the degree of similarity of distinct age measurements and examine heterogeneity within a detrital population (Galbraith, 1988, 1990). Radial plots allow simultaneous comparison of the age values of individual datapoints (defined by the intersection of a line projected from the origin through a particular point within the plot, to the arc age axis) and precision (as a percentage of the measured age, indicated on the horizontal axis). Examination of radial plots for the combined zircon (U–Th)/He and U/Pb datasets from sample 199453 analysed here (Fig. 3), highlights a number of important points:

(i) Distinct U/Pb analytical sessions are resolvable based on their dissimilar operational external precision during individual analytical sessions (Fig. 3). Overall, the superior precision of the U/Pb dating technique is apparent. Within U/Pb analytical sessions, the influence of U-concentration on analytical precision is apparent, with zircon grains exhibiting higher U-concentrations and greater radiogenic lead, subsequently having lower internal uncertainty.

(ii) The youngest statistically coherent zircon U/Pb age population yielded a (U–Th)/He age of 104 ± 6.1 Ma (MSWD = 0.6), which is in excellent agreement (Figs. 3, 4 and 7) with both biostratigraphic constraints and the U/Pb Concordia age of 105.8 ± 1.2 Ma (MSWD = 1.5; $n = 28$; Barham et al., 2016). These data indicate that the zircon grains rapidly cooled through the U/Pb and (U–Th)/He system closure temperatures essentially simultaneously and have not been exposed to any later resetting event. Despite variation in individual analyses for each of the two chronology techniques, age populations appear normally distributed and essentially define single

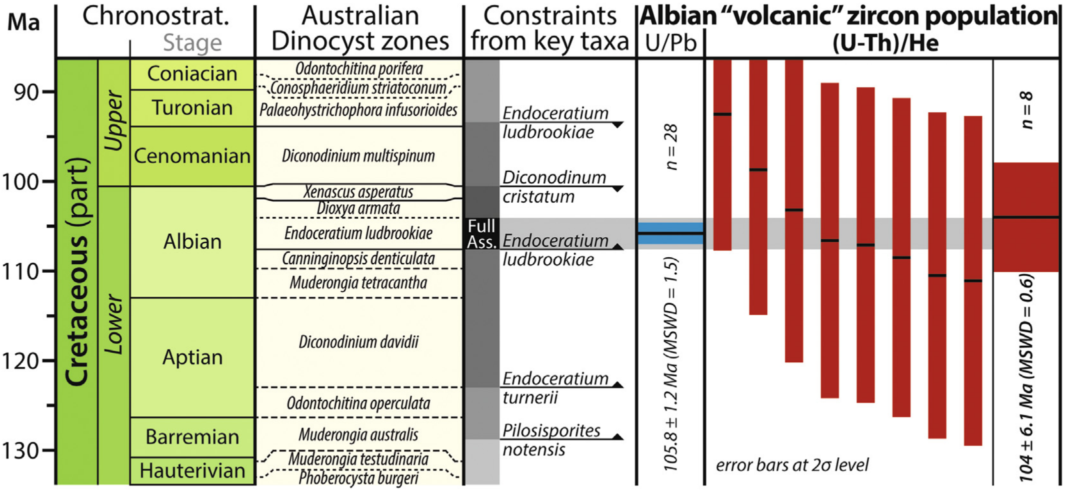

Figure 7. Integrated chronostratigraphic and biostratigraphic constraints provided by analyses for sample 199453. New (U–Th)/He data shown in red. Arrowheads indicate the first and last appearance of key taxa. Magnitude of grey within the biostratigraphic constraints corresponds to overlapping constraints from key taxa, with the continuous horizontal grey bar equating to the *Endoceratium ludbrookiae* biozone indicated by the "Full Ass." = full palynological assemblage. Chronostratigraphy modified from Gradstein et al. (2012), Australian dinocyst zonation from Partridge (2006), U/Pb data from Barham et al. (2016).

populations (Fig. 4). MSWD values associated with the respective dating approaches support recognition of discrete populations and give statistical confidence that the two dating systems represent temporally indistinguishable event/s (Wendt and Carl, 1991; Schoene et al., 2013; Spencer et al., 2016). Therefore, the grains were exposed to the Earth's surface rapidly and were not subsequently sufficiently buried to experience temperatures $>\sim 180$ °C prior to, or after, incorporation into the Madura Formation. Isolated zircon grain ages apparently postdate the host sediments deposition, a fact that attests more to the synsedimentary nature of the volcanism, tightness of age constraints and otherwise exceptional agreement of dating systems than inadequacies of the age constraints (dinocyst biostratigraphy, U/Pb geochronology and (U–Th)/He thermochronology). Previously identified differences between detrital zircon population age profiles of the Madura Shelf, Ceduna Subbasin and Eromanga Basin indicate significant distinction between their respective sedimentary systems (Barham et al., 2016, 2018). Collectively, these datasets all strongly support a volcanic origin and rapid, direct transport to the Madura Shelf catchment as opposed to any protracted erosion from deeper igneous systems and/or erosion from local volcaniclastics and subsequent surface transport processes with further episodes of intermediate burial and recycling.

(iii) (U–Th)/He ages from limited Proterozoic zircon grains yield Neoproterozoic and early Paleozoic dates that suggest a more complex cooling history with longer crustal residence (due to disparity with U/Pb crystallisation age; Fig. 4) or reheating to the zircon helium partial retention zone ($\sim$140–220 °C; Guenthner et al., 2013). The latter interpretation may indicate erosion from intermediate sedimentary basins (e.g., Officer Basin) that were active at these times (Fig. 4; Grey et al., 2005). Such recycling may have implications for the world-class heavy mineral deposits developed along Cenozoic shorelines on the southern margin of Australia, in the same region as this case study, which have been interpreted to involve extreme upgrading via recycling of zircon (Hou et al., 2011; Reid et al., 2013). Furthermore, though less sensitive than apatite, the preservation of Neoproterozoic and early Paleozoic zircon (U–Th)/He cooling ages argues against significant burial/resetting and exhumation events being widespread regionally in the Mesozoic (e.g., MacDonald et al., 2013).

5.3. *Trace-element insights to source region evolution*

Although debate continues as to the nature of Cretaceous eastern Australia volcanism (Whitsunday Volcanic Province; Bryan et al., 2012; Tucker et al., 2016), regardless of the preferred model, zircon grains from this margin should express a continental trace-element signature given the continental position of parental volcanic activity, incorporation of continental geochemical contamination and overall siliceous nature of the large igneous province (Fig. 1; Ewart et al., 1992; Norvick et al., 2001; Bryan et al., 2012).

Predominantly Jurassic, low volume mafic rift-related volcanics of the Coleraine Volcanic Group and Caserton Fm. have been recorded in the Otway and Gippsland basins (Geoscience Australia and the Australian Stratigraphy Commission, 2018). Further to the south, dolerites associated with the Ferrar LIP have been dated to $\sim$180 Ma and cover large areas of Tasmania (Burgess et al., 2015; Ware, 2018). However, Mesozoic volcanic centres are currently unknown from the Bight Basin on the designated non-volcanic southern margin of Australia, despite extensive seismic surveys of the drowned continental margin, which are capable of mapping Cenozoic volcanics (Schofield and Totterdell, 2008). Mid-Cretaceous volcaniclastics are developed in the Otway Basin (in particular the Strzelecki Group; Fig. 1). Otway Basin volcaniclastics were initially interpreted as deriving locally (Gleadow and Duddy, 1981; Duddy, 2016) and from active rifting (Felton, 1992). It is now recognised that rifting largely preceded deposition of the major volcaniclastic sequences in the Otway and Gippsland Basins, with strong evidence for volcaniclastic derivation from the same eastern Australian Whitsunday Volcanic Province that supplied the Eromanga Basin (Bryan et al., 1997; Constantine, 2001; Geoscience Australia, 2018). Thus, an eastern sourcing is now widely accepted (e.g., Blevin and Cathro, 2008; Tosolini et al., 2018) for Otway Basin volcaniclastics. The area between the Yilgarn and Gawler cratons (Fig. 1), including the Madura Shelf, is underlain by Proterozoic juvenile crust with oceanic affinities (Kirkland et al., 2017). Given (i) regional basement compositions, (ii) pronounced crustal thinning and ultimate mid-Cretaceous development of new oceanic crust along the southern margin of Australia (Müller et al., 2000; Veevers, 2000), and (iii) lack of other impetus for any possible volcanism, zircon grains from hypothetical local southern margin volcanics could reasonably be expected to have trace-element signatures with more juvenile oceanic-crust affinities (sensu

Grimes et al., 2007) than either a continental arc or intra-plate siliceous large igneous province, as suggested for eastern Australia.

Although enhanced zircon fertility is commonly associated with felsic crystalline rock units, zircon can be generated across a range of rock compositions from gabbroic oceanic crust to S-type granites (Grimes et al., 2007, 2015; Kaczmarek et al., 2008; Lissenberg et al., 2009; Hopkinson et al., 2017; Spencer et al., 2017, 2018). Consequently, zircon trace-element signatures can be used to assist differentiation of detrital zircon origins (Grimes et al., 2007, 2015). Trace-element data from the Albian volcanic zircon grains on the Madura Shelf are associated with continental geochemical signatures (Fig. 6). Hence, since no other appropriately aged volcanic centres are known, trace-element data further support that volcanic zircon grains on the Madura Shelf were derived from the Whitsunday Volcanic Province rather than any hypothetical volcanic system on the southern margin of Australia, where known Cenozoic magmatism is interpreted as mantle-derived (Meeuws et al., 2016).

5.4. *An integrated model and future testing*

While little evidence can be presented to support a local southern margin volcanic source for Albian zircon grains on the Madura Shelf, zircon geochronology and Hf-isotope geochemistry, sedimentology, and landscape evolution modelling have demonstrated a potentially viable mechanism of delivering material from the Whitsunday Volcanic Province to the Ceduna Delta (Lloyd et al., 2016; Veevers et al., 2016; Salles et al., 2017). The similar U/Pb age and Hf-isotopic character of zircon grains on the Madura Shelf, as well as their trace element geochemistry, support derivation from the Whitsunday Volcanic Province. However, unlike the Ceduna Delta material, the Madura Shelf Mesozoic zircon component is discrete and volumetrically subordinate, which, along with (i) a lack of shared characteristic zircon age signatures, (ii) a distinctiveness of Albian zircon grain shape, (iii) lack of burial resetting of (U–Th)/He ages, and (iv) indications of extremely rapid transport for the Albian zircon subpopulation (agreement of dating techniques), are all interpreted here to support a distinct transport mechanism consistent with distal projection of a volcanic component into the Madura Shelf catchment (Barham et al., 2016). Although individually equivocal, data that may further resolve this contentious matter include: (i) analysis of Albian sequences within the Ceduna Delta (once drilled), or elsewhere, to discriminate a volcanically projected component similar to that supported for the Madura Shelf (though it may be difficult to resolve in the Ceduna Subbasin that should contain only slightly older detrital volcanic material transported via the transcontinental drainage system), (ii) analysis of paleodrainage systems between the Madura Shelf and Eromanga Basin to establish where any drainage divide exists and understand if this was ever breached, (iii) more precise dating (chemical abrasion isotope dilution thermal ionisation mass spectrometry) of Albian zircon grains to better understand their crystallization histories, and (iv) investigation of lower temperature thermochronometers (e.g., apatite) to further interrogate the post-crystallization history of any potentially volcanic components.

6. Conclusions

Indistinguishable (U–Th)/He and U/Pb geochronology population ages of 104 ± 6.1 Ma and 105.8 ± 1.2 Ma, respectively, obtained from zircon grains hosted in the Madura Formation support rapid cooling as expected for volcanic grains. The ages are also identical to those suggested by the *Endoceratium ludbrookiae* dinocyst biozone assigned for that level of the stratigraphy, implying (i) accuracy of the current definitions of the chronostratigraphic interval and the decay constants for the two independent geochronometer systems, and (ii) rapid incorporation of the volcanic grains into the Madura Shelf sequence post crystallisation. A lack of younger (U–Th)/He ages argues against intermediate burial or thermal resetting and, in combination with existing data, supports the extreme volcanic dispersal of ~106 Ma zircon grains. New analyses of the trace-element composition of these Cretaceous zircon grains indicate a continental signature for the volcanic source region. This geochemistry is consistent with Hf-isotope fingerprinting of an eastern Australia continental volcanism source rather than a hypothetical, southern margin oceanic volcanic source.

Integrated zircon (U–Th)/He and U/Pb geochronology and trace-element geochemistry has significant potential to constrain sediment provenance and routing possibilities, as well as assist recognition of contemporaneous volcanic zircon grains within detrital populations and thus provide absolute ages of deposition. Therefore, multi-proxy age and geochemical data extractable from single grains following standard LA-ICPMS detrital zircon provenance work is proven to be a viable mechanism of interrogating the origins of discrete subpopulations. Although high uncertainties with the (U–Th)/He (~8%) and LA-ICPMS (~1%–4%) techniques will decrease the ability of these analytical approaches to confidently prove genuine synchronicity of closure ages (volcanic populations) in older samples, potential re-setting of the (U–Th)/He age in consideration of the U/Pb crystallization age still yields greater constraints on grain history and regional geology (sediment burial, orogeny, regional igneous activity etc.) than single dating approaches alone.

Acknowledgements

The authors thank Nick Roberts, Carl Spandler, Scott Bryan and an anonymous reviewer for comments that variously helped improve and clarify this manuscript. GeoHistory Facility instruments were funded via an Australian Geophysical Observing System grant provided to AuScope Pty Ltd. by the AQ44 Australian Education Investment Fund program. Part of this research was undertaken using the EM instrumentation (ARC LE130100053) at the John de Laeter Centre, Curtin University. M.D. was supported by ARC Discovery funding scheme (DP160102427), Curtin Research Fellowship and Australian Scientific Instruments Pty Ltd. M.D. thanks C. May for help with solution ICP-MS analyses, I. Dunkl for sharing PepiFLEX software for ICP-MS data reduction and A. Frew for help with zircon dissolution.

Appendix A. Supplementary data

Supplementary data to this article can be found online at https://doi.org/10.1016/j.gsf.2019.01.003.

References

Barham, M., Kirkland, C.L., Reynolds, S., O'Leary, M.J., Evans, N.J., Allen, H., Haines, P.W., Hocking, R.M., McDonald, B.J., Belousova, E., Goodall, J., 2016. The answers are blowin' in the wind: ultra-distal ashfall zircons, indicators of Cretaceous super-eruptions in eastern Gondwana. Geology 44, 643–646.

Barham, M., Reynolds, S., Kirkland, C.L., O'Leary, M.J., Evans, N.J., Allen, H.J., Haines, P.W., Hocking, R.M., McDonald, B.J., 2018. Sediment routing and basin evolution in Proterozoic to Mesozoic east Gondwana: a case study from southern Australia. Gondwana Research 58, 122–140.

Belousova, E., Griffin, W., O'Reilly, S.Y., Fisher, N., 2002. Igneous zircon: trace element composition as an indicator of source rock type. Contributions to Mineralogy and Petrology 143, 602–622.

Blakey, R.C., 2008. Gondwana paleogeography from assembly to breakup – A 500 m.y. odyssey. In: Fielding, C.R., Frank, T.D., Isbell, J.L. (Eds.), Resolving the Late Paleozoic Ice Age in Time and Space. The Geological Society of America, Special Paper 441, Boulder, Colorado, pp. 1–28.

Blevin, J.E., Cathro, D.L., 2008. Australian Southern Margin Synthesis, Project GA707, pp. 1–104.

Blundy, J., Wood, B., 1994. Prediction of crystal–melt partition coefficients from elastic moduli. Nature 372, 452.

Boynton, W.V., 1984. Chapter 3 - cosmochemistry of the rare Earth elements: meteorite studies. In: Henderson, P. (Ed.), Developments in Geochemistry. Elsevier, pp. 63–114.

Bryan, S.E., Constantine, A.E., Stephens, C.J., Ewart, A., Schön, R.W., Parianos, J., 1997. Early Cretaceous volcano-sedimentary successions along the eastern Australian continental margin: implications for the break-up of eastern Gondwana. Earth and Planetary Science Letters 153, 85–102.

Bryan, S.E., Cook, A.G., Allen, C.M., Siegel, C., Purdy, D.J., Greentree, J.S., Uysal, I.T., 2012. Early-mid cretaceous tectonic evolution of eastern Gondwana: from silicic LIP magmatism to continental rupture. Episodes 35, 142–152.

Bryan, S.E., Ewart, A., Stephens, C.J., Parianos, J., Downes, P.J., 2000. The Whitsunday Volcanic Province, Central Queensland, Australia: lithological and stratigraphic investigations of a silicic-dominated large igneous province. Journal of Volcanology and Geothermal Research 99, 55–78.

Bryan, S.E., Peate, I.U., Peate, D.W., Self, S., Jerram, D.A., Mawby, M.R., Marsh, J.S., Miller, J.A., 2010. The largest volcanic eruptions on Earth. Earth Science Reviews 102, 207–229.

Buret, Y., von Quadt, A., Heinrich, C., Selby, D., Wälle, M., Peytcheva, I., 2016. From a long-lived upper-crustal magma chamber to rapid porphyry copper emplacement: reading the geochemistry of zircon crystals at Bajo de la Alumbrera (NW Argentina). Earth and Planetary Science Letters 450, 120–131.

Burgess, S.D., Bowring, S.A., Fleming, T.H., Elliot, D.H., 2015. High-precision geochronology links the Ferrar large igneous province with early-Jurassic ocean anoxia and biotic crisis. Earth and Planetary Science Letters 415, 90–99.

Campbell, I.H., Reiners, P.W., Allen, C.M., Nicolescu, S., Upadhyay, R., 2005. He–Pb double dating of detrital zircons from the Ganges and Indus Rivers: implication for quantifying sediment recycling and provenance studies. Earth and Planetary Science Letters 237, 402–432.

Cawood, P.A., Hawkesworth, C.J., Dhuime, B., 2012. Detrital zircon record and tectonic setting. Geology 40, 875–878.

Cawood, P.A., Nemchin, A.A., Freeman, M., Sircombe, K., 2003. Linking source and sedimentary basin: detrital zircon record of sediment flux along a modern river system and implications for provenance studies. Earth and Planetary Science Letters 210, 259–268.

Cecil, M.R., Ducea, M.N., Reiners, P., Gehrels, G., Mulch, A., Allen, C., Campbell, I., 2010. Provenance of Eocene river sediments from the central northern Sierra Nevada and implications for paleotopography. Tectonics 29, TC6010. https://doi.org/10.1029/2010TC002717.

Chapman, J.B., Gehrels, G.E., Ducea, M.N., Giesler, N., Pullen, A., 2016. A new method for estimating parent rock trace element concentrations from zircon. Chemical Geology 439, 59–70.

Constantine, A.E., 2001. Sedimentology, Stratigraphy and Palaeoenvironment of the Upper Jurassic-Lower Cretaceous Non-marine Strzelecki Group, Gippsland Basin, Southeastern Australia. Department of Earth Sciences. Monash University, Melbourne, Australia.

Corfu, F., Hanchar, J.M., Hoskin, P.W.O., Kinny, P., 2003. Atlas of zircon textures. Reviews in Mineralogy and Geochemistry 53, 469.

Danišík, M., Štěpančíková, P., Evans, N.J., 2012. Constraining long-term denudation and faulting history in intraplate regions by multisystem thermochronology: an example of the Sudetic Marginal Fault (Bohemian Massif, central Europe). Tectonics 31.

Dickinson, W.R., Gehrels, G.E., 2009. Use of U–Pb ages of detrital zircons to infer maximum depositional ages of strata: a test against a Colorado Plateau Mesozoic database. Earth and Planetary Science Letters 288, 115–125.

Dickinson, W.R., Gehrels, G.E., 2010. Insights into north American paleogeography and paleotectonics from U–Pb ages of detrital zircons in Mesozoic strata of the Colorado plateau, USA. International Journal of Earth Sciences 99, 1247–1265.

Direen, N.G., Borissova, I., Stagg, H.M.J., Colwell, J.B., Symonds, P.A., 2007. Nature of the continent–ocean transition zone along the southern Australian continental margin: a comparison of the Naturaliste Plateau, SW Australia, and the central Great Australian Bight sectors. Geological Society London Special Publications 282, 239–263.

Direen, N.G., Stagg, H.M.J., Symonds, P.A., Colwell, J.B., 2008. Architecture of volcanic rifted margins: new insights from the Exmouth – gascoyne margin, Western Australia. Australian Journal of Earth Sciences 55, 341–363.

Direen, N.G., Stagg, H.M.J., Symonds, P.A., Colwell, J.B., 2011. Dominant symmetry of a conjugate southern Australian and East Antarctic magma-poor rifted margin segment. Geochemistry, Geophysics, Geosystems 12, Q02006. https://doi.org/10.1029/2010GC003306.

Duddy, I.R., 2003. Mesozoic. In: Birch, W.D. (Ed.), Geology of Victoria. Geological Society of Australia Special Publication, vol. 23, pp. 239–289.

Duddy, I.R., 2016. Gondwana-wide thermotectonic events and their expression in southern and south-eastern Australia before and after break-up: denudation, volcanism, sedimentation and provenance. In: Grosser, M. (Ed.), 2016 Selwyn Symposium. Supercontinents Assembly through Break-Up: An eastern Gondwana Perspective. The Geological Society of Australia - Victoria Division. The University of Melbourne, pp. 39–41.

Ewart, A., Schon, R.W., Chappell, B.W., 1992. The Cretaceous volcanic-plutonic province of the central Queensland (Australia) coast—a rift related 'calc-alkaline' province. Earth and Environmental Science Transactions of the Royal Society of Edinburgh 83, 327–345.

Farley, K.A., Wolf, R.A., Silver, L.T., 1996. The effects of long alpha-stopping distances on (U-Th)/He ages. Geochimica et Cosmochimica Acta 60, 4223–4229.

Fedo, C.M., Sircombe, K.N., Rainbird, R.H., 2003. Detrital zircon analysis of the sedimentary record. Reviews in Mineralogy and Geochemistry 53, 277–303.

Felton, E.A., 1992. Sedimentary History of the Early Cretaceous Otway Group, Otway Basin. Department of Geology. The University of Wollongong, Australia.

Fielding, L., Najman, Y., Millar, I., Butterworth, P., Ando, S., Padoan, M., Barfod, D., Kneller, B., 2017. A detrital record of the Nile River and its catchment. Journal of the Geological Society 174, 301–317.

Fisher, R.V., 1961. Proposed classification of volcaniclastic sediments and rocks. GSA Bulletin 72, 1409–1414.

Fisher, R.V., Schmincke, H.-U., 1984. Pyroclastic Rocks. Spinger-Verlag, Berlin.

Gagnevin, D., Daly, J.S., Kronz, A., 2010. Zircon texture and chemical composition as a guide to magmatic processes and mixing in a granitic environment and coeval volcanic system. Contributions to Mineralogy and Petrology 159, 579–596.

Galbraith, R.F., 1988. Graphical display of estimates having differing standard errors. Technometrics 30, 271–281.

Galbraith, R.F., 1990. The radial plot: graphical assessment of spread in ages. International Journal of Radiation Applications and Instrumentation Part D Nuclear Tracks and Radiation Measurements 17, 207–214.

Gallagher, K., Dumitru, T.A., Gleadow, A.J.W., 1994. Constraints on the vertical motion of eastern Australia during the Mesozoic. Basin Research 6, 77–94.

Gallagher, K., Lambeck, K., 1989. Subsidence, sedimentation and sea-level changes in the Eromanga Basin, Australia. Basin Research 2, 115–131.

Gehrels, G., 2014. Detrital zircon U-Pb geochronology applied to tectonics. Annual Review of Earth and Planetary Sciences 42, 127–149.

Geoscience Australia, 2018. Otway Basin. Geoscience Australia.

Geoscience Australia and the Australian Stratigraphy Commission, 2018. Australian Stratigraphic Units Database. Geoscience Australia and Australian Stratigraphy Commission.

Gibbons, A.D., Whittaker, J.M., Müller, R.D., 2013. The breakup of East Gondwana: assimilating constraints from Cretaceous ocean basins around India into a best-fit tectonic model. Journal of Geophysical Research Solid Earth 118, 808–822.

Gleadow, A.J.W., Duddy, I.R., 1981. Early Cretaceous volcanism and the early break-up history of southeastern Australia: evidence from fission track dating of volcaniclastic sediments. In: Gondwana Five: Selected Papers and Abstracts, fifth Gondwana symposium, pp. 295–300.

Gradstein, F.M., Ogg, J.G., Schmitz, M., Ogg, G., 2012. The Geologic Time Scale 2012. Elsevier, Amsterdam, the Netherlands.

Greentree, J., 2011. Palaeoenvironmental Setting of Dinosaur Trackways in the Context of the Closing Stages of Eromanga Basin Evolution. Queensland University of Technology, Brisbane, Australia, p. 107.

Grey, K., Hocking, R.H., Stevens, M.K., Bagas, L., Carlsen, G.M., Irimies, F., Pirajno, F., Haines, P.W., Apak, S.N., 2005. Lithostratigraphic Nomenclature of the Officer Basin and Correlative Parts of the Paterson Orogen, Western Australia.

Grimes, C.B., John, B.E., Kelemen, P.B., Mazdab, F.K., Wooden, J.L., Cheadle, M.J., Hanghøj, K., Schwartz, J.J., 2007. Trace element chemistry of zircons from oceanic crust: a method for distinguishing detrital zircon provenance. Geology 35, 643–646.

Grimes, C.B., Wooden, J.L., Cheadle, M.J., John, B.E., 2015. "Fingerprinting" tectono-magmatic provenance using trace elements in igneous zircon. Contributions to Mineralogy and Petrology 170, 1–26.

Guenthner, W.R., Reiners, P.W., Ketcham, R.A., Nasdala, L., Giester, G., 2013. Helium diffusion in natural zircon: radiation damage, anisotropy, and the interpretation of zircon (U-Th)/He thermochronology. American Journal of Science 313, 145–198.

Haq, B.U., 2014. Cretaceous eustasy revisited. Global and Planetary Change 113, 44–58.

Heiken, G., 1985. Volcanic Ash. University of California Press, Los Alamos, USA.

Helby, R., Morgan, R., Partridge, A.D., 1987. A palynological zonation of the Australian Mesozoic. In: Jell, P.A. (Ed.), Studies in Australian Mesozoic Palynology. Memoir Association Australasian Palaeontologists, pp. 1–94.

Hopkinson, T.N., Harris, N.B.W., Warren, C.J., Spencer, C.J., Roberts, N.M.W., Horstwood, M.S.A., Parrish, R.R., Eimf, 2017. The identification and significance of pure sediment-derived granites. Earth and Planetary Science Letters 467, 57–63.

Hou, B., Keeling, J., Reid, A., Fairclough, M., Wairland, I., Belousova, E., Frakes, L., Hocking, R., 2011. Heavy mineral sands in the Eucla Basin, Southern Australia: depositional and province-scale prospectivity. Economic Geology 106, 687–712.

Ito, H., Spencer, C.J., Danišík, M., Hoiland, C.W., 2017. Magmatic tempo of Earth's youngest exposed plutons as revealed by detrital zircon U-Pb geochronology. Scientific Reports 7, 12457.

Kaczmarek, M.-A., Müntener, O., Rubatto, D., 2008. Trace element chemistry and U–Pb dating of zircons from oceanic gabbros and their relationship with whole rock composition (Lanzo, Italian Alps). Contributions to Mineralogy and Petrology 155, 295–312.

Kirkland, C.L., Daly, J.S., Whitehouse, M.J., 2007. Provenance and terrane evolution of the kalak nappe complex, Norwegian caledonides: implications for neoproterozoic paleogeography and tectonics. The Journal of Geology 115, 21–41.

Kirkland, C.L., Smithies, R.H., Spaggiari, C.V., Wingate, M.T.D., Quentin de Gromard, R., Clark, C., Gardiner, N.J., Belousova, E.A., 2017. Proterozoic crustal evolution of the Eucla basement, Australia: implications for destruction of oceanic crust during emergence of Nuna. Lithos 278–281, 427–444.

Laurie, J.R., Bodorkos, S., Nicoll, R.S., Crowley, J.L., Mantle, D.J., Mory, A.J., Wood, G.R., Backhouse, J., Holmes, E.K., Smith, T.E., Champion, D.C., 2016. Calibrating the middle and late Permian palynostratigraphy of Australia to the geologic timescale via U–Pb zircon CA-IDTIMS dating. Australian Journal of Earth Sciences 63, 701–730.

Lissenberg, C.J., Rioux, M., Shimizu, N., Bowring, S.A., Mével, C., 2009. Zircon dating of oceanic crustal accretion. Science 323, 1048–1050.

Lloyd, J., Collins, A.S., Payne, J.L., Glorie, S., Holford, S., Reid, A.J., 2016. Tracking the Cretaceous transcontinental Ceduna River through Australia: the hafnium isotope record of detrital zircons from offshore southern Australia. Geoscience Frontiers 7, 237–244.

Lowry, D.C., 1970. In: Australia, G.S.o.W. (Ed.), Geology of the Western Australian Part of the Eucla Basin. Geological Survey of Western Australia, Perth, p. 207.

Ludwig, K.R., 2012. User's manual for isoplot/Ex, v.3.75, A Geochronological Toolkit for Microsoft Excel, vol. 5. Berkeley Geochronological Center Special Publications.

MacDonald, J.D., Holford, S.P., Green, P.F., Duddy, I.R., King, R.C., Backé, G., 2013. Detrital zircon data reveal the origin of Australia's largest delta system. Journal of the Geological Society 170, 3–6.

Makulini, P., Kirkland, C.L., Barham, M., 2018. Zircon grain shape holds provenance information; a case study from southwestern Australia. Geological Journal 1–15.

Mami, T., Kenji, H., Kenichiro, T., Takeyoshi, Y., Tomokazu, H., Shoichi, K., 2017. Timescale of magma chamber processes revealed by U–Pb ages, trace element contents and morphology of zircons from the Ishizuchi caldera, Southwest Japan Arc. Island Arc 26, e12182.

Markwitz, V., Kirkland, C.L., 2018. Source to sink zircon grain shape: constraints on selective preservation and significance for Western Australian Proterozoic basin provenance. Geoscience Frontiers 9, 415–430.

Markwitz, V., Kirkland, C.L., Mehnert, A., Gessner, K., Shaw, J., 2017. 3-D characterization of detrital zircon grains and its implications for fluvial transport, mixing, and preservation bias. Geochemistry, Geophysics, Geosystems 18, 4655–4673.

Matthews, K.J., Hale, A.J., Gurnis, M., Müller, R.D., DiCaprio, L., 2011. Dynamic subsidence of eastern Australia during the cretaceous. Gondwana Research 19, 372–383.

McKenzie, N.R., Smye, A.J., Hegde, V.S., Stockli, D.F., 2018. Continental growth histories revealed by detrital zircon trace elements: a case study from India. Geology 46, 275–278.

Meeuws, F.J.E., Holford, S.P., Foden, J.D., Schofield, N., 2016. Distribution, chronology and causes of Cretaceous – Cenozoic magmatism along the magma-poor rifted southern Australian margin: Links between mantle melting and basin formation. Marine and Petroleum Geology 73, 271–298.

Menzies, M.A., Klemperer, S.L., Ebinger, C.J., Baker, J., 2002. Characteristics of volcanic rifted margins. In: Menzies, M.A., Klemperer, S.L., Ebinger, C.J., Baker, J. (Eds.), Volcanic Rifted Margins. Geological Society of America.

Metcalfe, I., Crowley, J.L., Nicoll, R.S., Schmitz, M., 2015. High-precision U-Pb CA-TIMS calibration of Middle Permian to Lower Triassic sequences, mass extinction and extreme climate-change in eastern Australian Gondwana. Gondwana Research 28, 61–81.

Mihut, D., Müller, R.D., 1998. Volcanic margin formation and mesozoic rift propagators in the cuvier abyssal plain off western Australia. Journal of Geophysical Research Solid Earth 103, 27135–27149.

Mory, A.J., Crowley, J.L., Backhouse, J., Nicoll, R.S., Bryan, S.E., López Martínez, M., Mantle, D.J., 2017. Apparent conflicting Roadian–Wordian (middle permian) CA-IDTIMS and palynology ages from the canning basin, western Australia. Australian Journal of Earth Sciences 64, 889–901.

Müller, R.D., Flament, N., Matthews, K.J., Williams, S.E., Gurnis, M., 2016. Formation of Australian continental margin highlands driven by plate–mantle interaction. Earth and Planetary Science Letters 441, 60–70.

Müller, R.D., Gaina, C., Clark, S., 2000. Seafloor spreading around Australia. In: Veevers, J. (Ed.), Billion-year Earth History of Australia and Neighbours in Gondwanaland. Gemoc Press, Sydney, Australia, pp. 18–28.

Norvick, M.S., Smith, M.A., Power, M.R., 2001. The plate tectonic evolution of eastern australasia guided by the stratigraphy of the Gippsland basin. In: Hill, K.C., Bernecker, T. (Eds.), Eastern Australasian Basins Symposium: A Refocused Energy Perspective for the Future. Petroleum Exploration Society of Australia, Special Publications, Melbourne, pp. 15–24.

Olierook, H.K.H., Barham, M., Fitzsimons, I.C.W., Timms, N.E., Jiang, Q., Evans, N.J., McDonald, B.J., 2019. Tectonic controls on sediment provenance evolution in rift basins: detrital zircon U–Pb and Hf isotope analysis from the Perth Basin, Western Australia. Gondwana Research 66, 126–142.

Olierook, H.K.H., Jourdan, F., Merle, R.E., Timms, N.E., Kusznir, N., Muhling, J.R., 2016. Bunbury Basalt: Gondwana breakup products or earliest vestiges of the Kerguelen mantle plume? Earth and Planetary Science Letters 440, 20–32.

Olierook, H.K.H., Timms, N.E., Wellmann, J.F., Corbel, S., Wilkes, P.G., 2015. 3D structural and stratigraphic model of the Perth Basin, Western Australia: implications for sub-basin evolution. Australian Journal of Earth Sciences 62, 447–467.

Partridge, A.D., 2006. Late Cretaceous palynology zonations for Australia. In: Monteil, E. (Ed.), Australian Mesozoic and Cenozoic Palynology Zonations – Updated to the 2004 Geologic Timescale. Geoscience Australia, p. 8.

Pirajno, F., Hoatson, D.M., 2012. A review of Australia's Large Igneous Provinces and associated mineral systems: implications for mantle dynamics through geological time. Ore Geology Reviews 48, 2–54.

Playford, P.E., Cockbain, A.E., Low, G.H., 1976. Geology of the Perth Basin, western Australia, vol. 124. Geological Survey of Western Australia Bulletin, Perth, Australia.

Pointon, M.A., Chew, D.M., Ovtcharova, M., Sevastopulo, G.D., Crowley, Q.G., 2012. New high-precision U–Pb dates from western European Carboniferous tuffs; implications for time scale calibration, the periodicity of late Carboniferous cycles and stratigraphical correlation. Journal of the Geological Society 169, 713–721.

Pointon, M.A., Chew, D.M., Ovtcharova, M., Sevastopulo, G.D., Delcambre, B., 2014. High-precision U–Pb zircon CA-ID-TIMS dates from western European late Viséan bentonites. Journal of the Geological Society 171, 649–658.

Rahl, J.M., Reiners, P.W., Campbell, I.H., Nicolescu, S., Allen, C.,M., 2003. Combined single-grain (U-Th)/He and U/Pb dating of detrital zircons from the Navajo Sandstone, Utah. Geology 31, 761–764.

Rasmussen, B., Fletcher, I.R., 2010. Dating sedimentary rocks using in situ U-Pb geochronology of syneruptive zircon in ash-fall tuffs <1 mm thick. Geology 38, 299–302.

Reid, A., Keeling, J., Boyd, D., Belousova, E., Hou, B., 2013. Source of zircon in world-class heavy mineral placer deposits of the Cenozoic Eucla Basin, southern Australia from LA-ICPMS U–Pb geochronology. Sedimentary Geology 286–287, 1–19.

Reiners, P.W., Campbell, I.H., Nicolescu, S., Allen, C.M., Hourigan, J.K., Garver, J.I., Mattinson, J.M., Cowan, D.S., 2005. (U-Th)/(He-Pb) double dating of detrital zircons. American Journal of Science 305, 259–311.

Reiners, P.W., Spell, T.L., Nicolescu, S., Zanetti, K.A., 2004. Zircon (U-Th)/He thermochronometry: He diffusion and comparisons with ^{40}Ar/^{39}Ar dating. Geochimica et Cosmochimica Acta 68, 1857–1887.

Salles, T., Flament, N., Müller, D., 2017. Influence of mantle flow on the drainage of eastern Australia since the Jurassic Period. Geochemistry, Geophysics, Geosystems 18, 280–305.

Sano, Y., Tsutsumi, Y., Terada, K., Kaneoka, I., 2002. Ion microprobe U–Pb dating of Quaternary zircon: implication for magma cooling and residence time. Journal of Volcanology and Geothermal Research 117, 285–296.

Saylor, J.E., Stockli, D.F., Horton, B.K., Nie, J., Mora, A., 2012. Discriminating rapid exhumation from syndepositional volcanism using detrital zircon double dating: implications for the tectonic history of the Eastern Cordillera, Colombia. GSA Bulletin 124, 762–779.

Schmitz, M.D., 2012. Radiogenic isotope geochronology. In: Gradstein, F., Ogg, J.G., Schmitz, M., Ogg, G. (Eds.), The Geological Timescale. Elsevier, Amsterdam, pp. 115–127.

Schoene, B., Condon, D.J., Morgan, L., Mclean, N., 2013. Precision and accuracy in geochronology. Elements 9, 19–24.

Schofield, A., Totterdell, J., 2008. Distribution, Timing and Origin of Magmatism in the Bight and Eucla Basins, p. 19.

Seton, M., Müller, R.D., Zahirovic, S., Gaina, C., Torsvik, T., Shephard, G., Talsma, A., Gurnis, M., Turner, M., Maus, S., Chandler, M., 2012. Global continental and ocean basin reconstructions since 200Ma. Earth-Science Reviews 113, 212–270.

Sircombe, K.N., Freeman, M.J., 1999. Provenance of detrital zircons on the Western Australia coastline—implications for the geologic history of the Perth basin and denudation of the Yilgarn craton. Geology 27, 879–882.

Spencer, C.J., Cavosie, A.J., Raub, T.D., Rollinson, H., Jeon, H., Searle, M.P., Miller, J.A., McDonald, B.J., Evans, N.J., The Edinburgh Ion Microprobe Facility, 2017. Evidence for melting mud in Earth's mantle from extreme oxygen isotope signatures in zircon. Geology 45, 975–978.

Spencer, C.J., Danišík, M., Ito, H., Hoiland, C., Tapster, S., Jeon, H., McDonald, B., Evans, N.J., 2019. Rapid exhumation of Earth's youngest exposed granites driven by subduction of an oceanic arc. Geophysical Research Letters 46. https://doi.org/10.1029/2018GL080579.

Spencer, C.J., Kirkland, C.L., Roberts, N.M.W., 2018. Implications of erosion and bedrock composition on zircon fertility: examples from South America and Western Australia. Terra Nova 30, 289–295.

Spencer, C.J., Kirkland, C.L., Taylor, R.J.M., 2016. Strategies towards statistically robust interpretations of in situ U–Pb zircon geochronology. Geoscience Frontiers 7, 581–589.

Stagg, H.M.J., Cockshell, C.D., Willcox, J.B., Hill, A.J., Needham, D.J.L., Thomas, B., O'Brien, G.W., Hough, L.P., 1990. Basins of the Great Australian Bight Region: Geology and Petroleum Potential. Bureau of Mineral Resources. Continental Margins Program Folio 5.

Suthren, R.J., 1985. Facies analysis of volcaniclastic sediments: a review. Geological Society, London, Special Publications 18, 123–146.

Tosolini, A.-M.P., Korasidis, V.A., Wagstaff, B.E., Cantrill, D.J., Gallagher, S.J., Norvick, M.S., 2018. Palaeoenvironments and palaeocommunities from lower cretaceous high-latitude sites, Otway Basin, southeastern Australia. Palaeogeography, Palaeoclimatology, Palaeoecology 496, 62–84.

Totterdell, J.M., Bradshaw, B.E., 2004. The structural framework and tectonic evolution of the Bight Basin. In: Boult, P.J., Johns, D.R., Lang, S.C. (Eds.), Eastern Australasian Basins Symposium II. Petroleum Exploration Society of Australia, Special Publication, pp. 41–61.

Totterdell, J.M., Krassay, A.A., 2003. Sequence stratigraphic correlation of onshore and offshore Bight Basin successions. Geoscience Australia Record 2003/02, 50 pp.

Trail, D., Bruce Watson, E., Tailby, N.D., 2012. Ce and Eu anomalies in zircon as proxies for the oxidation state of magmas. Geochimica et Cosmochimica Acta 97, 70–87.

Tucker, R.T., Roberts, E.M., Henderson, R.A., Kemp, A.I.S., 2016. Large igneous province or long-lived magmatic arc along the eastern margin of Australia during the Cretaceous? Insights from the sedimentary record. The Geological Society of America Bulletin 128, 1461–1480.

Tucker, R.T., Roberts, E.M., Hu, Y., Kemp, A.I.S., Salisbury, S.W., 2013. Detrital zircon age constraints for the Winton formation, Queensland: contextualizing Australia's late cretaceous dinosaur faunas. Gondwana Research 24, 767–779.

Veevers, J.J., 2000. Change of tectono-stratigraphic regime in the Australian plate during the 99 Ma (mid-Cretaceous) and 43 Ma (mid-Eocene) swerves of the Pacific. Geology 28, 47–50.

Veevers, J.J., Belousova, E.A., Saeed, A., 2016. Zircons traced from the 700–500 Ma transgondwanan supermountains and the gamburtsev subglacial mountains to the ordovician lachlan orogen, cretaceous Ceduna delta, and modern channel country, central-southern Australia. Sedimentary Geology 334, 115–141.

Veevers, J.J., Saeed, A., Belousova, E.A., Griffin, W.L., 2005. U–Pb ages and source composition by Hf-isotope and trace-element analysis of detrital zircons in Permian sandstone and modern sand from southwestern Australia and a review of the paleogeographical and denudational history of the Yilgarn Craton. Earth Science Reviews 68, 245–279.

Vermeesch, P., 2009. RadialPlotter: aJava application for fission track, luminescence and other radial plots. Radiation Measurements 44, 409–410.

Vermeesch, P., 2012. On the visualisation of detrital age distributions. Chemical Geology 312–313, 190–194.

Ware, B., 2018. Large Igneous Provinces of the Southern Hemisphere: Isotopic Geochemistry and Plagioclase and Pyroxene $^{40}Ar/^{39}Ar$ Geochronology of the Kalkarindji, Karoo and Ferrar Provinces. Department of Applied Geology. Curtin University, Perth, Western Australia, p. 419.

Wendt, I., Carl, C., 1991. The statistical distribution of the mean squared weighted deviation. Chemical Geology Isotope Geoscience Section 86, 275–285.

Xu, J., Stockli, D.F., Snedden, J.W., 2017. Enhanced provenance interpretation using combined U–Pb and (U–Th)/He double dating of detrital zircon grains from lower Miocene strata, proximal Gulf of Mexico Basin, North America. Earth and Planetary Science Letters 475, 44–57.